SYNTHESIS AND CHARACTERIZATION OF NOVEL HIGHLY SWELLABLE ANTIMICROBIAL STARCH HYDROGELS IMPREGNATED WITH ZnO NANOPARTICLES AS EDIBLE FOOD COATING

NAHED A. ABD EL-GHANY,[*] NADIA A. MOHAMED[**] and ZAIN M. MAHMOUD[*]

[*]*Department of Chemistry, Faculty of Science, Cairo University, Giza, 12613, Egypt*
[**]*Department of Chemistry, College of Science, Qassim University, Buraidah 51452, Saudi Arabia*
✉ *Corresponding authors: N. A. Abd El-Ghany, abdelghanyn@sci.cu.edu.eg*
N. A. Mohamed, na.ahmed@qu.edu.sa

Received April 14, 2025

The growing resistance of microbes towards conventional antibiotics is the driving force for finding out alternative antimicrobial agents that can work by mechanisms different from that of classical antibiotics. For this, in this study, new cross-linked St-g-PMPA/PCL hydrogels were prepared via chemical grafting/crosslinking of starch (St) with N-(4-methoxyphenyl)acrylamide (MPA) and different concentrations (3, 5, 10% based on St mass) of diallyldimethylammonium chloride (CL) using $(NH_4)_2S_2O_8$/$NaHSO_3$ as a redox initiator. This was followed by the impregnation of zinc oxide nanoparticles (ZnONPs) at 1 and 3 wt% ratios into St-g-PMPA/PCL-3%, getting St-g-PMPA/PCL-3%/ZnONPs-1% and St-g-PMPA/PCL-3%/ZnONPs-3% composites, respectively. Various analytical techniques were employed to confirm the chemical structures of the prepared hydrogels and composites. Their inhibition performance against the tested microbes can be ordered as follows: St-g-PMPA/PCL-3%/ZnONPs-3% > St-g-PMPA/PCL-3%/ZnONPs-1% > St-g-PMPA/PCL-3% > St-g-PMPA, whereas the virgin St did not show antimicrobial action. The St-g-PMPA/PCL-3%/ZnONPs-3% composite behaves as a good barrier for the coated green bell peppers, preserving them from microbial contamination and retarding their spoilage, in comparison with uncoated peppers. The material was found to be safe for normal human lung fibroblast cells. The incorporation of MPA, CL, and ZnONPs into St developed its microbial inhibition performance, providing a good approach to produce promising antimicrobial coating materials.

Keywords: starch, hydrogels, ZnONPs, synthesis, antimicrobial activity, green peppers preservation, cytotoxicity

INTRODUCTION

Hydrogels are, essentially, a cross-linked hydrophilic three-dimensional polymeric network, able to absorb huge quantities of biological fluids and water. Crosslinking may take place via physical or chemical bonds.[1] They are used for many applications in fighting microbes,[2] drug delivery,[3] tissue engineering,[4] wastewater treatment,[5] and food industry.[6] Recently, there has been a tendency to displace synthetic hydrogels, which are non-renewable, hard to degrade, and have high production costs, by hydrogels of natural origin (environmentally green ones).[7]

Polysaccharides, which have a long-chain polymer structure made up of monosaccharides linked by glycosidic bonds, are found in a variety of organisms, including algae, plants, microorganisms, and animals. They are essential in biological systems, facilitating cell-cell communication, molecular recognition within the immune system, and processes such as tumor metastasis and mitogenesis.[8] Natural polysaccharides exhibit a wide range of biological activities, including anti-tumor, immune modulation, antioxidant, and anti-inflammatory properties, which contribute to their growing popularity.[9] Plant polysaccharides are characterized by strong intermolecular interactions, resulting in a stable structure that is highly resistant to pH and temperature changes. These polymers provide a variety of health benefits, making them valuable in health product formulations. They have a variety of physical, chemical, and biological properties, including antioxidant activity and potential therapeutic

effects on metabolic diseases. Furthermore, their strong hydrophilicity improves their ability to interact with water and other substances, whereas high viscosity can influence the texture and stability of formulations.[10] Among polysaccharides, starch-based hydrogels have gained huge attention due to easy availability and applications. Moreover, they are non-toxic, biocompatible, and cheap. For these reasons, they can be alternatives to synthetic hydrogels.

Starch is found in some cereals and root vegetables, such as maize (corn), rice, wheat, potato, and cassava. Amylose and amylopectin are the major constituents of starch; they are organized in a semi-crystalline structure in the starch grains.[11] Amylose has a linear structure of α-D-glucose units bonded to each other by α(1→4) glycosidic bonds, while amylopectin has highly branched structure of short α-1,4 glucose chains, which are bonded by α-1,6 branch linkages. Starch has attracted great attention in biomedical applications, such as wound dressings and drug delivery, due to its advantages including biodegradability, renewability, nontoxicity, and low cost.[12] Unprocessed starch does not have antimicrobial properties; this issue has been addressed by impregnating antimicrobial substances into the starch backbone. The combination of starch with other materials can improve the antimicrobial performance of starch-based materials, broadening the field of its applications. Starch can be functionalized with specific groups like guanidine or quaternary ammonium, as well as combined with metal nanoparticles, to afford antimicrobial features.[13]

Zinc oxide (ZnO) is a most common and widely used additive in various fields, such as in food packaging, cosmetics, bio-medicine, agriculture, and coatings, as it is abundant in nature, low cost, biocompatible, pigment-free, hydrophobic, UV absorbing, and antimicrobial properties.[14,15]

Starch is used in edible films and coatings as it has the capacity to form colorless, tasteless, and translucent layers, with properties similar to those of synthetic polymers.[16] It has been demonstrated that nanostructured ZnO can inhibit the growth of bacteria and fungi, extending the shelf life of foods.[17-19] Starch and its derivatives are generally modified by chemical, physical and biotechnological methods.[20] Among them, grafting with vinyl or acrylic monomers, which is achieved by first generating free radicals on the starch backbone, which then serve as macro initiators for vinyl or acrylic monomers.[21] Cationic starch can be obtained through grafting with cationic monomers,[22] and the cationic groups are generally amino, immonium, ammonium, sulphonium and phosphonium. Generally, they have been synthesized by grafting quaternary ammonium salt onto the starch backbone.[23]

Starch/gelatin/octenyl succinic anhydride hydrogel microspheres showed potential applications to modify the texture of food products and to encapsulate flavor or bioactive compounds.[24] Corn starch hydrogel microspheres and alginate-pectin produced bioactive films for food preservation.[25] Corn starch granules were physically modified with a high-speed shear homogenizer for hydrogel and film production, and good functional properties were obtained, with improved water resistance and water barrier property, the material showing potential for application in the food packaging sector.[26] Corn starch/polyvinyl alcohol hydrogel loaded with silver nanoparticles/linseed oil polyol for film preparation has been applied for antimicrobial packaging.[27] Polyacrylamide/starch composite hydrogel with improved swelling properties was applied as potential material for controlled drug delivery applications for gastrointestinal administration and local treatment of infections.[28] Starch-g-polyacrylamide-co-polylactic acid hydrogel exhibited antibacterial and antioxidant properties and swelled up to 481% at pH 7.20. It is non-toxic, biodegradable, and particularly suitable as a material for wound dressings.[29] Starch/ZnONPs/glycerol edible film showed enhanced water resistance, tensile strength, elongation percentage, and biodegradability.[30]

In the present paper, three cationic hydrogels were synthesized by chemical grafting copolymerization/crosslinking of starch (St) using N-(4-methoxyphenyl)acrylamide (MPA) and different amounts of diallyldimethylammonium chloride (CL) crosslinker, obtaining St-g-PMPA/PCL-3%, St-g-PMPA/PCL-5%, and St-g-PMPA/PCL-10% hydrogels. Further, two different amounts of ZnONPs (1 and 3% based on hydrogel weight) were loaded into the matrix of St-g-PMPA/PCL-3% to form St-g-PMPA/PCL-3%/ZnONPs-1% and St-g-PMPA/PCL-3%/ZnONPs-3% composites, respectively. Their chemical, inner, and surface structures were characterized using suitable analytical methods. Their swelling behavior at different pH conditions, antimicrobial activity, preservation

impact on green bell peppers, and cytotoxicity were also studied.

EXPERIMENTAL

Materials

Nasr Chemical Co. (Egypt) provided the starch (St) containing 25% amylose and 75% amylopectin. p-Anisidine and diallyldimethylammonium chloride (CL) were obtained from Loba Chemie (India). Sigma-Aldrich (Germany) supplied all the solvents, reagents, and chemicals, which were used exactly as received. The Micro Analytical Center (Cairo University) provided the microorganisms for studying antibacterial and antifungal activities.

Experimental methods

Synthesis of N-(4-Methoxyphenyl)acrylamide (MPA)

Acryloyl chloride (0.05 mol/L) was added dropwise to a p-anisidine solution (0.05 mol/L dissolved in DMF) and then stirred on a magnetic stirrer in an ice bath for 3 hours. After the reaction was complete, crushed ice was added to the resulting mixture to precipitate the product N-(4-methoxyphenyl)acrylamide (MPA). The solid product was filtered and washed several times with cold water, then recrystallized from hot water for complete purification, and allowed to dry in an oven at 60 °C for 8 hours; the preparation reaction is shown in Scheme 1.

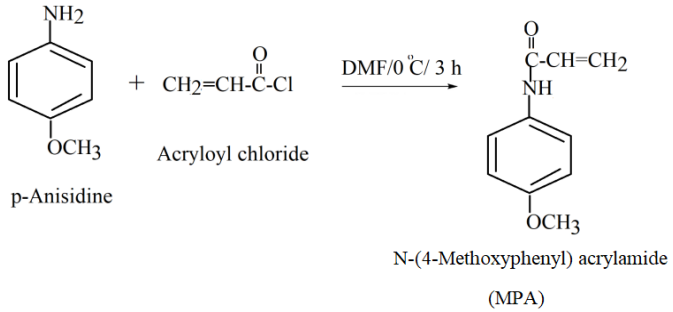

Scheme 1: Preparation of MPA

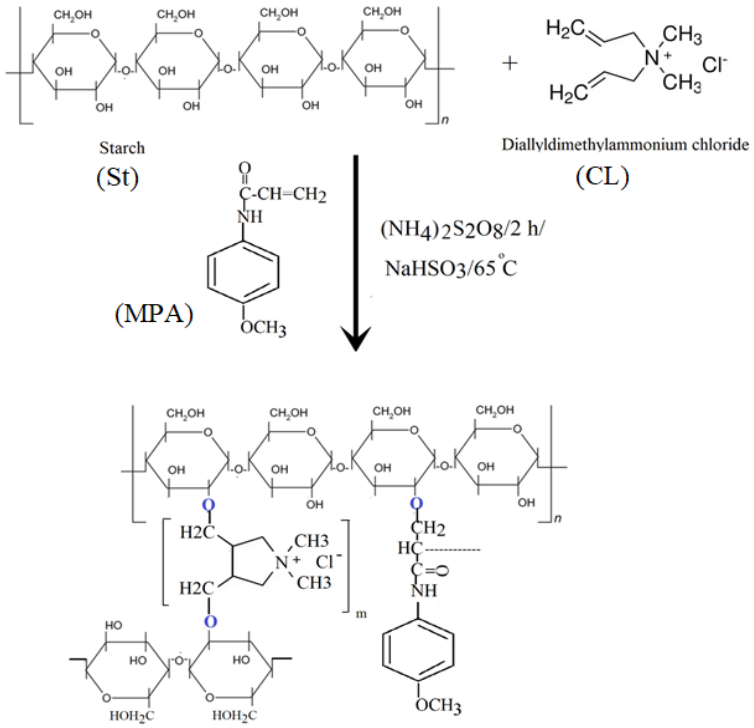

Scheme 2: Preparation method of St-g-PMPA/PCL hydrogels

Synthesis of cross-linked St-g-PMPA/PCL hydrogels

Graft copolymerization of St with both MPA monomer and different amounts of CL was performed as previously reported.[23] Dry corn St (1.0 g) dissolved in 50 mL double-distilled water was heated at 85 °C for 30 minutes with stirring to produce gelatinized St. The temperature was then reduced to 65 °C, and the calculated amounts of MPA (0.25 mol/L) and the

cross-linker CL (3, 5, and 10% based on St mass) were gradually added to the reaction mixture. The flask was provided with nitrogen gas, and the grafting process was started by slowly adding a suitable amount of $(NH_4)_2S_2O_8/NaHSO_3$ (3×10^{-2} mol/L) as a redox initiator. After 2 hours, the hydrogels were precipitated on cold methanol and stirred overnight to drain water before being collected by filtration and then washed with methanol several times and allowed to dry in an oven at 65 °C for 8 h. Three hydrogels (based on the amount of cross-linker used) were created and named St-g-PMPA/PCL-3%, St-g-PMPA/PCL-5%, and St-g-PMPA/PCL-10%, as shown in Scheme 2. A Soxhlet was used for 8 h to extract the homopolymer from the grafted polymer by using methanol as a solvent. Lastly, Equations (1) – (3) were used to determine the percent graft (% G), percent grafting efficiency (% GE), and percent homopolymer (% H), as indicated in Table 1:

$$\% G = [W_2 - W_o / W_o] \times 100 \quad (1)$$

$$\% GE = [W_1 - W_o / W_2 - W_o] \times 100 \quad (2)$$

$$\% H = [W_1 - W_2 / W_3] \times 100 \quad (3)$$

where W_o is the initial St weight, W_1 and W_2 are the weights of grafted St before and after Soxhlet extraction, respectively, and W_3 is the weight of the monomers consumed, as illustrated in Table 1.

Table 1
Graft copolymerization data of St-g-PMPA copolymer and its hydrogels

Sample	% G	% GE	% H
St-g-PMPA	190	90.4	9.1
St-g-PMPA/PCL-3%	200	93.1	6.7
St-g-PMPA/PCL-5%	180	90.2	9.3
St-g-PMPA/PCL-10%	166	87.4	10.85

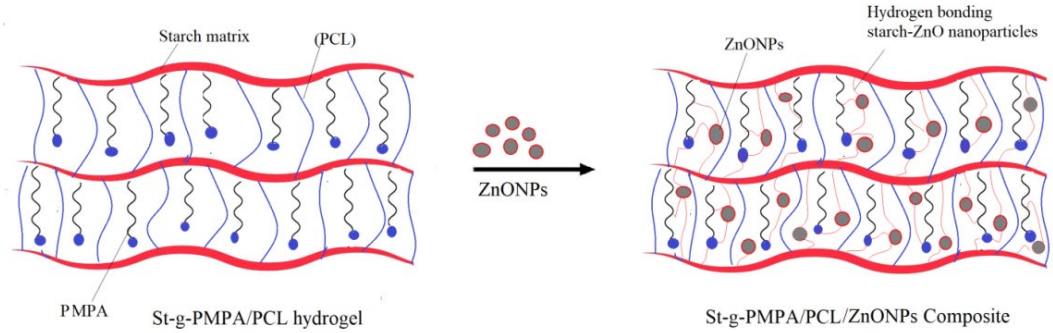

Figure 1: Schematic presentation of St-g-PMPA/PCL-3%/ZnONPs composites

Synthesis of St-g-PMPA/PCL-3%/ZnONPs composites

The nanocomposites were prepared through blending 1 g of St-g-PMPA/PCL-3% hydrogel with different concentrations of the ZnONPs (1 and 3% based on hydrogel weight), producing two nanocomposites designated as St-g-PMPA/PCL-3%/ZnONPs-1% and St-g-PMPA/PCL-3%/ZnONPs-3%, respectively. The ZnONPs were held inside the hydrogel matrix via hydrogen bonds with the polymeric chains, resulting in uniform distribution of the nanoparticles, as depicted in Figure 1.

Swelling behavior of St-g-PMPA/PCL hydrogels in different pH media

The swelling capability of the St-g-PMPA/PCL-3%, St-g-PMPA/PCL-5%, and St-g-PMPA/PCL-10% hydrogels was performed as follows: a predetermined weight of the dry hydrogel specimen was immersed in a buffer solution of pH 4, 7, and 9, and remained at room temperature as a function of time until equilibrium was achieved. The swellability percentage was calculated using Equation (4):

$$\% \text{ Swell ability} = [W_1 - W_o / W_o] \times 100 \quad (4)$$

where W_o and W_1 are the weights of the hydrogel sample before and after swelling, respectively. The measurements were taken in triplicate, and the estimated error was within 1%.[21,31,32]

Antimicrobial assay

The colony forming unit counting test (CFU) was used to check how well the St-g-PMPA copolymer, St-g-PMPA/PCL-3% hydrogel, St-g-PMPA/PCL-3%/ZnONPs-1%, and St-g-PMPA/PCL-3%/ZnONPs-3% composites worked against certain germs, specifically *S. aureus*, *E. coli*, and *C. albicans*. The antimicrobial ratio of the samples was determined by cultivating and incubating a suspension of microbes (McFarl and standard 0.5) in Mueller-Hinton broth medium. The microbial suspension (200 µL), the samples, and the DMSO control sample were added to

a 96-well plate. The plates with dried nutrient agar and microbial solutions (20 µL) were incubated at 37 °C for 24 hours. A digital camera was used to inspect the microbial colonies on the plates and count them. Equation (5)[33] was used to measure the antimicrobial performance.

$$\textit{Antibacterial ratio (\%)} = \frac{(\text{№ CFUs in control} - \text{№ CFUs in exp. sample}) \times 100\%}{\text{№ CFUs in control}} \quad (5)$$

Cytotoxicity evaluation using viability assay

To conduct the cytotoxicity test, normal human lung fibroblast cells (WI-38 cells) were seeded in 96-well plates with 1×10^4 cells per well in 100 µL of growth medium. After 24 h of seeding, fresh medium with varying concentrations of the St-g-PMPA/PCL-3%/ZnONPs-3% composite was added. The latter compound was tested by adding serial two-fold dilutions to confluent cell monolayers in 96-well microtiters flat bottoms. Microtiter plates were incubated at 37 °C in a humidified incubator with 5% CO_2 for 24 h. Following incubation, the percent of the viable cells was determined using a colorimetric method, the MTT test, as previously described.[34] Equation (6) was used to calculate the total number of viable cells and their percentage:

$$\% \text{ Viable cells} = [ODt/ODc] \times 100\% \quad (6)$$

where ODt and ODc are the mean optical density of wells after and before treatment with the tested sample. The optical density was measured at 590 nm with the microplate reader (SunRise, TECAN, Inc, USA).

Plotting the relationship between surviving cells and tested sample concentrations yields a survival curve for the cell line after treatment with the sample. The cytotoxic concentration (CC_{50}), which causes toxic effects in 50% of intact cells, was estimated using Graphpad Prism Software (San Diego, CA, USA).[35]

Preservation test of green bell peppers

Fresh green bell peppers were coated with a suspended solution of St-g-PMPA/PCL-3% hydrogel and St-g-PMPA/PCL-3%/ZnONPs-3% composite (62.5 µg mL^{-1}, in distilled water) using a spreading technique. For comparison, uncoated pepper was used under identical conditions. A digital camera was used to record the changes in shape and freshness of peppers over a period of 1-16 days.[6]

Measurements

Fourier transform infrared (FTIR) spectroscopy

An FTIR spectrophotometer (Model 8000, Japan) was used to investigate the chemical structures of the St, MPA, St-g-PMPA copolymer, St-g-PMPA/PCL-3% hydrogel, and St-g-PMPA/PCL-3%/ZnONPs-3% composite. The samples were ground with KBr and compressed at 400 kg/cm² hydraulic pressure to form pellets. Spectra were measured in the 400-4000 cm^{-1} range.

X-ray diffraction (XRD) analysis

A Brucker's D-8 Advanced Wide-Angle X-Ray Diffractometer was used to record XRD patterns of the St, gelatinized St, and St-g-PMPA/PCL-3% and St-g-PMPA/PCL-5% hydrogels, and St-g-PMPA/PCL-3%ZnONPs-1%, and St-g-PMPA/PCL-3%/ZnONPs-3% composites at room temperature. Nickel-filtered CuKα radiation (40 kV, 30 mA) produces X-rays of a wavelength of 1.5406° A. The sample was placed on a sample holder and examined in the reflection mode at an angle of 2θ from 4° to 70° at a speed of 8° min^{-1}.

Scanning electron microscopy (SEM)

The surface morphology of the St granules, gelatinized St, and St-g-PMPA/PCL-3% and St-g-PMPA/PCL-10% hydrogels, and St-g-PMPA/PCL-3%ZnONPs-1%, and St-g-PMPA/PCL-3%/ZnONPs-3% composites was investigated using a Hitachi Scanning Electron Microscope (Model S-450) equipped with an energy dispersive X-ray spectrometer (EDS). Before investigation, the dried specimens were placed on the surface of an aluminum Scanning Electron Microscopy sample holder and covered with gold. The used accelerating voltage was 20 kV.

Transmission electron microscopy (TEM)

The suspended solution of the St-g-PMPA/PCL-3%/ZnONPs-3% composite was examined using a transmission electron microscope (Type JEM-HR-JEOL-JEM 2100) to visualize the size and dispersion of the ZnONPs.

RESULTS AND DISCUSSION

Characterization of St-g-PMPA/PCL hydrogels and ZnONPs biocomposites

FTIR analysis

Figure 2 presents the FTIR spectra of free St, MPA, and St-g-PMPA copolymer. The spectrum of St exhibited the following distinctive bands: at 3441 and 2935 cm^{-1}, corresponding to OH and CH groups stretching vibrations, respectively, the small intensity peak at 1654 cm^{-1} related to the contaminated protein and fat, the band at 1451 cm^{-1} due to the bending vibration of the CH_2 groups, and those at 1180, 1100, and 1035 cm^{-1} attributed to C-O-C and C-OH, respectively. In addition, the peak at 860 cm^{-1} was assigned to the glucopyranose ring.[36,37]

The PMA spectrum illustrated some distinguishable stretching vibration peaks: at 3310 cm^{-1} related to the NH, at 3070 cm^{-1} corresponding to the aliphatic and aromatic CH groups, at 2970 and 2850 cm^{-1} due to CH_3, at 1670 ascribed to CO-NH, and at 1524 and 1460 cm^{-1} assigned to C=C (aliphatic and aromatic) overlapping with the bending vibration of the -

NH and -CH_3 groups. The additional peaks appearing at 1256, 1190, and 840 cm^{-1} were related to the ph-O, -OCH_3, and p-substituted benzene ring, respectively.

The FTIR spectrum of the St-g-PMPA copolymer showed a broad peak around 3430 cm^{-1} due to the overlapped stretching vibrations of NH of the MPA and OH of the St. This is in addition to the appearance of the peaks at 1670 cm^{-1} (CO-NH), at 1530 and 1460 cm^{-1} (C=C (aromatic), at 1265 cm^{-1} (ph-O), at 1170 cm^{-1} (-OCH_3), and at 835 cm^{-1} (p-substituted benzene ring) due to the incorporation of MPA into St, which confirms the grafting process.

The spectrum of the St-g-PMPA/PCL-3% hydrogel (as a representative example of the hydrogels) showed the appearance of a new peak at 1380 cm^{-1} due to the additional free CH_3 groups of the crosslinker PCL. The St-g-PMPA/PCL-3%/ZnONPs-3% composite spectrum showed shifting of many functional group vibrations to lower frequencies as a result of the electrostatic interaction and hydrogen bonding between ZnONPs and the hydrogel functional groups, as illustrated in Figure 3.

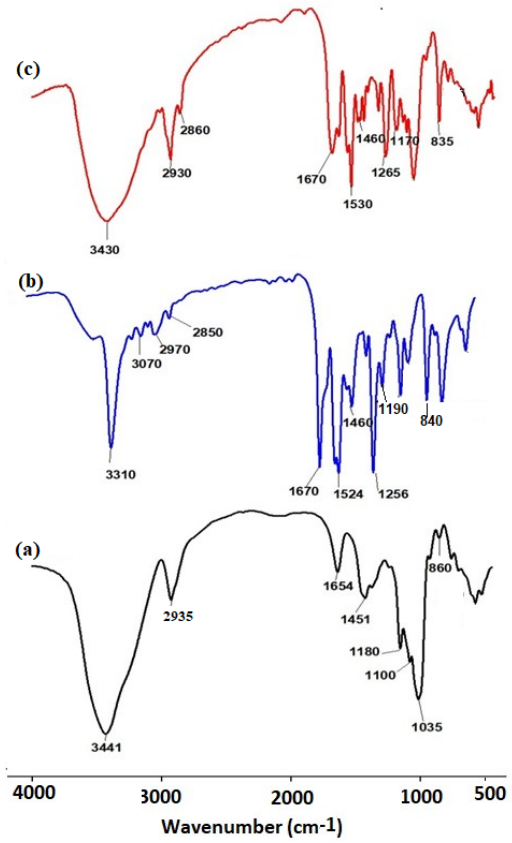

Figure 2: FTIR spectra of: (a) St, (b) MPA, and (c) St-g-PMPA copolymer

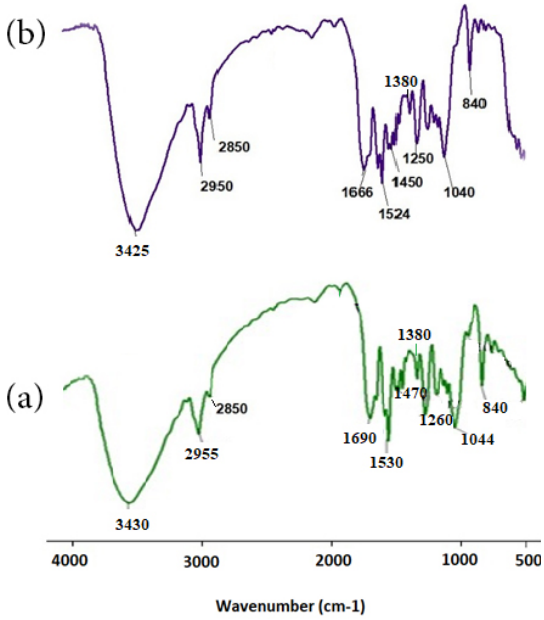

Figure 3: FTIR spectra of: (a) St-g-PMPA/PCL-3% hydrogel, and (b) St-g-PMPA/PCL-3%/ZnONPs-3% composite

XRD analysis

The inner structure of the modified St was investigated using the XRD technique. Figure 4 shows the XRD patterns of native St, gelatinized St, and St-g-PMPA/PCL-3% and St-g-PMPA/PCL-5% hydrogels. The XRD pattern of St illustrated a crystalline nature, represented by the prominent peaks at 2θ = 15.2°, 18.2°, 19.2°, 21.5°, and 23.2°, while the inner structure of gelatinized St appeared as semi-crystalline, as indicated by the diminishing of St crystalline peaks, the broadness of the peak around 21° and the appearance of a new peak at 27.3°.[23]

Grafting of MPA and CL molecules on the St resulted in the breakage of the inter- and intramolecular hydrogen bonds, thus separating the chains from each other, leading to an amorphous structure indicated by the broad peak around 2θ = 21°. These results confirm the synthesis of St-g-PMPA/PCL hydrogels. The increase in the amount of the cross-linker resulted in an increase in the amorphous fractions due to

the breakage of greater amounts of the internal hydrogen bonds.

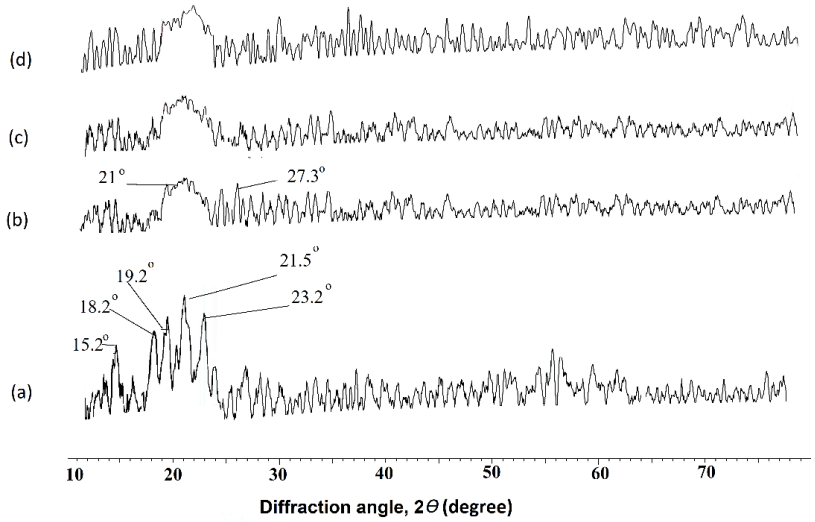

Figure 4: XRD analysis of: (a) St, (b) gelatinized St, (c) St-g-PMPA/PCL-3% hydrogel, and (d) St-g-PMPA/PCL-5% hydrogel

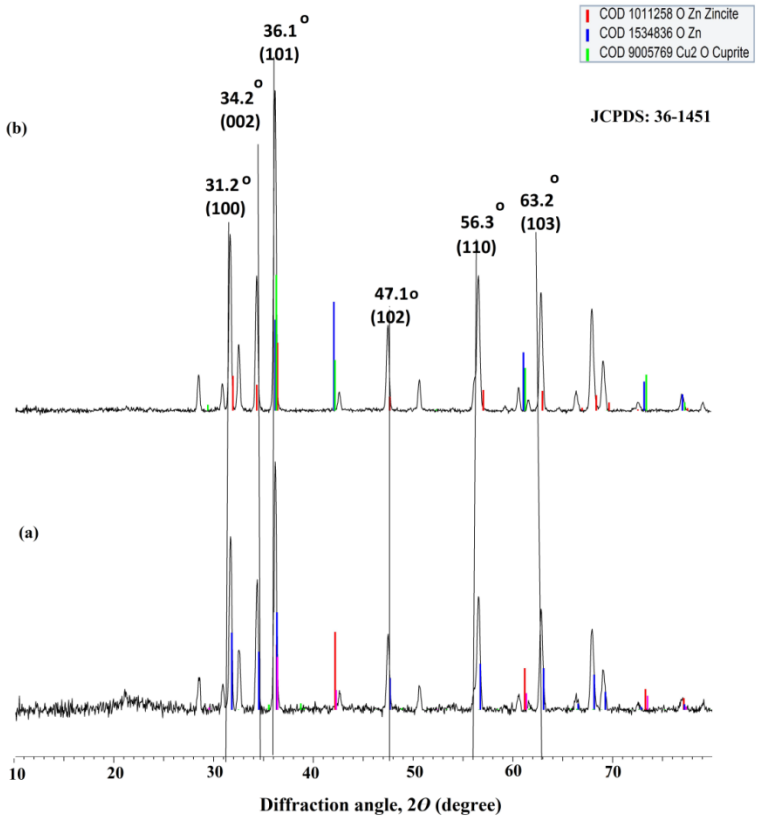

Figure 5: XRD patterns of: (a) St-g-PMPA/PCL-3%/ZnONPs-1% composite and (b) St-g-PMPA/PCL-3%/ZnONPs-3% composite

The XRD patterns of St-g-PMPA/PCL-3%/ZnONPs-1% and St-g-PMPA/PCL3%/ZnONPs-3% composites displayed a completely amorphous structure, as indicated by the disappearance of St crystalline peaks. This might be due to the destruction of the

residual hydrogen bonding between St-g-PMPA/PCL-3% chains by the action of the impregnated ZnONPs, in addition to their chelation with the OH, NH, CO and OCH_3 groups of the St-g-PMPA/PCL-3% hydrogel. The patterns showed new peaks at 2θ = 31.2°, 34.2°, 36.1°, 47.1°, 56.3° and 63.2°, which corresponded to zincite (ZnONPs) crystal planes (100), (002), (101), (102), (110) and (103), respectively (ref. code JCPDS 36-1451).[38] The intensity of these peaks increased as a function of ZnONPs content of the composites, as illustrated in Figure 5.

SEM observation

SEM observation was used to investigate the surface morphology of St before and after modification. Figure 6 shows that the granular St's surface morphology appeared smooth and crystallite, whereas gelatinized St had a rough surface and an open structure. The grafting process resulted in the breakage of a large number of inter- and intramolecular hydrogen bonds that bound the St chains together, leading to a highly amorphous and porous structure as illustrated in the SEM images of the St-g-PMPA/PCL hydrogels. The images also showed a homogeneous distribution of pores in the hydrogel's matrix, and the number of pores increased as the crosslinking concentration increased from St-g-PMPA/PCL-3% to St-g-PMPA/PCL-10%. The SEM images also showed homogeneous distribution of the ZnONPs on the surface of the PMPA/PCL-3%/ZnONPs-1% and PMPA/PCL-3%/ZnONPs-3% composites.

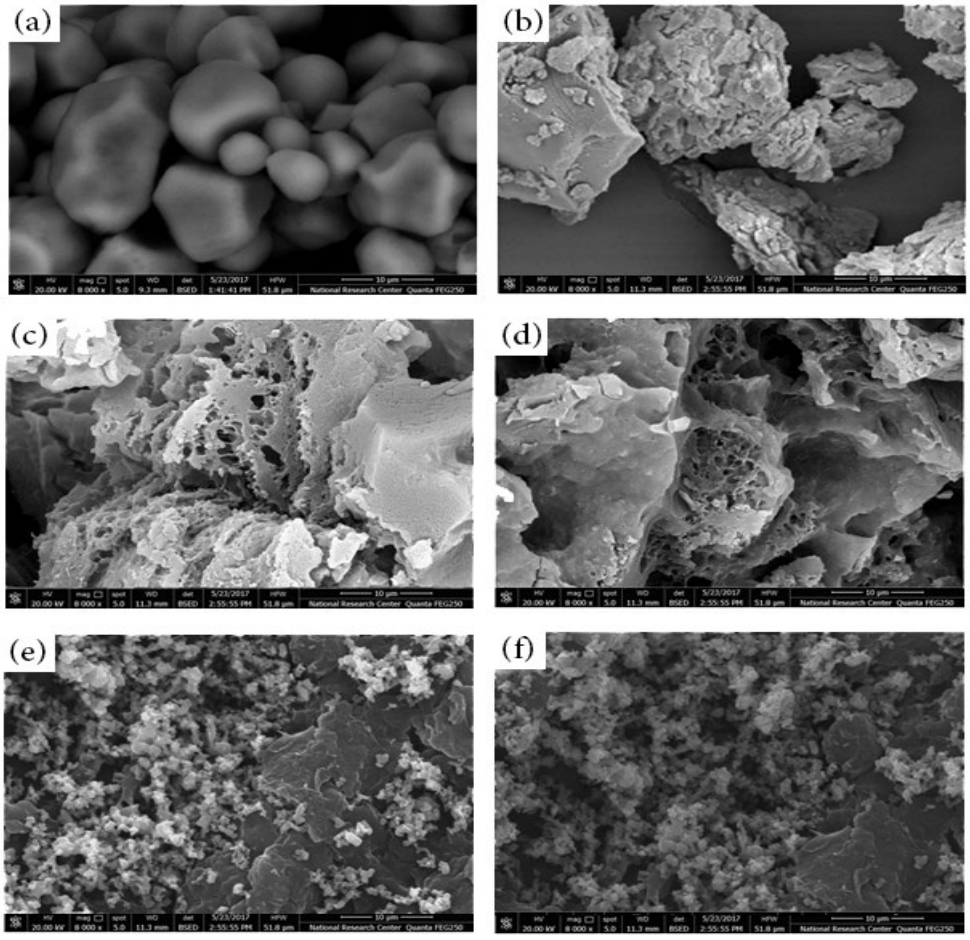

Figure 6: SEM images of (a) St granules, (b) gelatinized St, (c) St-g-PMPA/PCL-3% hydrogel, (d) St-g-PMPA/PCL-10% hydrogel, (e) St-g-PMPA/PCL-3%/ZnONPs-1% composite, and (f) St-g-PMPA/PCL-3%/ZnONPs-3% composite at 8000x magnification

EDS analysis

The percentage of the C, O, N, and Zn elements that constituted the St-g-PMPA/PCL-3%/ZnONPs-3% composite (as a representative example) was evidenced by EDS analysis (Fig. 7).

TEM analysis

TEM analysis was used to display the shape and the size of the nanoparticles inside the St-g-PMPA/PCL-3%/ZnONPs-3% composite. The ZnONPs appeared spherical with particle size ranging from 14 to 33.85 nm. The images also showed homogeneous distribution of the ZnONPs in the composite matrix, as illustrated in Figure 8.

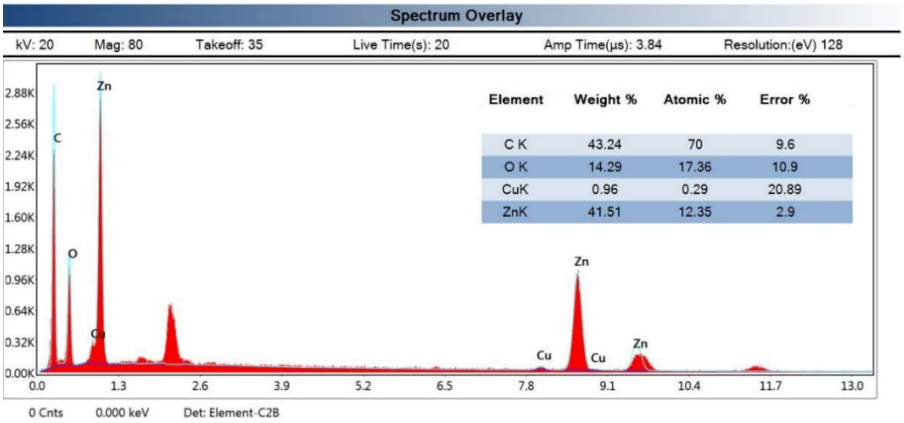

Figure 7: EDS analysis of St-g-PMPA/PCL-3%/ZnONPs-3% composite

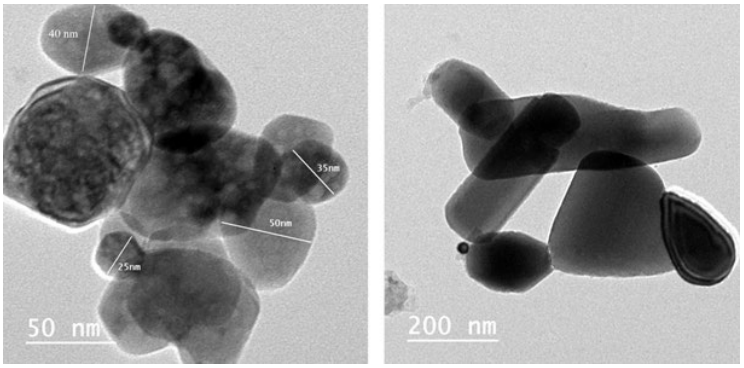

Figure 8: TEM micrographs of St-g-PMPA/PCL-3%/ZnONPs-3% composite at different magnifications

Swelling behavior of St-g-PMPA/PCL hydrogels

The ability to swell is a favorable characteristic of polymer hydrogels. Its investigation has a great importance, mainly due to the impact of the swelling behavior on the surface properties, mobility, solute transfer mechanism, and mechanical features of the hydrogels.

In order to investigate the sensitivity of the St-g-PMPA/PCL hydrogels to pH, their swelling capacity was studied at various pH (4, 7, and 9) over various time intervals at 25 °C (Fig. 9). The results showed that the swellability of the hydrogels in acidic (pH = 4) and neutral (pH = 7) buffer solutions increased up to 6 h before leveling off. Meanwhile, in basic medium (pH = 9), the swellability decreased over time. It was observed that the swelling behavior of the hydrogels could be attributed to osmotic pressure imbalances within the hydrogel caused by the repulsive force interaction between the similarly charged $N^{+}(CH_3)_2$ groups present on the hydrogel backbone, resulting in extensive liquid diffusion into the hydrogel matrix.[23]

The swellability in acidic medium is greater than in neutral medium and basic medium, which could be attributed to protonation of the hydrogel's functional groups NH, CO, and OCH_3, resulting in an increase in the positive charge inside the hydrogels and, as a result, an increase in repulsive force interaction. While in a neutral medium, the high swellability was caused by hydrogen bonding between the methoxy ($-OCH_3$) groups and incoming water molecules, which resulted in an increase in the amount of bound water and thus high swellability.[39]

In contrast, the swellability in basic medium decreased over time. This could be due to the

shielding of the cross-linker $N^{+}(CH_3)_2$ groups with the base molecules, reducing their repulsive force interaction, decreasing their mobility inside the hydrogel, and lowering liquid diffusion into the hydrogel matrix.[40]

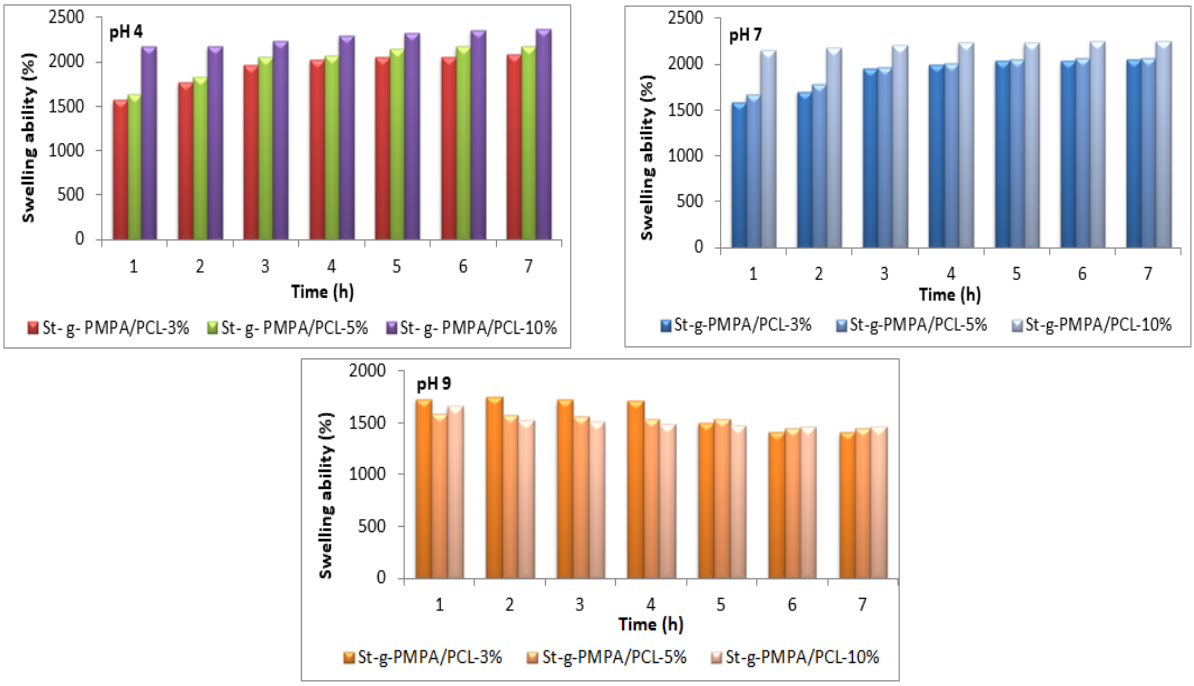

Figure 9: Swelling behavior of St-g-PMPA/PCL hydrogels in different pH media at 25 °C

It is worth noting that the degree of swelling increased as the amount of cross-linker increased, due the increased number of functional groups and pores, allowing for rapid liquid diffusion within the hydrogel matrix.

Antimicrobial analysis

The antimicrobial activities of the St-g-PMPA copolymer, St-g-PMPA/PCL-3% hydrogel (as a representative example), and St-g-PMPA/PCL-3%/ZnONPs-1% and St-g-PMPA/PCL-3%/ZnONPs-3% composites against Gram-positive bacteria (*S. aureus*), Gram-negative bacteria (*E. coli*), and fungi (*C. albicans*) were studied using the colony-forming unit counting test (CFU).[6,41] Native St had no observable antimicrobial property; therefore, the modification process imparted antimicrobial behavior to the material. Tables 2-4 show that the nanocomposites displayed a higher inhibition percent against the tested microbes than the other samples; and their inhibition activity increased with increasing the ZnONPs content. The order of their antimicrobial activity was: St-g-PMPA/PCL-3%/ZnONPs-3% > St-g-PMPA/PCL-3%/ZnONPs-1% > St-g-PMPA/PCL-3% > St-g-PMPA, whereas the strongest derivative PMPA/PCL-3%/ZnONPs-3% showed antimicrobial activities of 76.92, 68.57, and 65.17% against *S. aureus*, *E. coli* and *C. albicans*, respectively, compared to 58.46, 51.43, and 57.83% exhibited by the copolymer St-g-PMPA based on the number of dead colonies. Figure 10 displays photographs showing the antimicrobial activity of the tested samples against *S. aureus*, *E. coli* and *C. albicans*. It is worth mentioning that the higher antimicrobial activity of the nanocomposites results from the interaction between the ZnONPs and the microbial cell membrane. This interaction resulted in: (i) damage of the cell membrane and releasing of the cell components, (ii) production of reactive oxygen species (ROS), such as superoxide ($O^{2\bullet-}$), hydroxyl ($OH^{\bullet}$), hydrogen peroxide (H_2O_2), and singlet oxygen (O^2),[42] (iii) combination with the DNA, preventing RNA formation,[43] and (iv) inactivation of enzyme activity. Figure 11 illustrates a schematic representation of the

interaction between the ZnONPs and the microbial cell membrane.

Table 2
Antimicrobial activity of St-g-PMPA copolymer, St-g-PMPA/PCL-3% hydrogel and St-g-PMPA/PCL-3%/ZnONPs composites against *S. aureus*

S. aureus	St-g-PMPA	St-g-PMPA/PCL-3%	St-g-PMPA/PCL-3%/ZnONPs-1%	St-g-PMPA/PCL-3%/ZnONPs-3%	Control[a]
Dilution factor	10^{-4}	10^{-4}	10^{-4}	10^{-4}	10^{-4}
Volume of broth plated (µL)	20 µL	20 µL	20 µL	20 µL	20 µL
Colony forming unit (CFU) at the dilution factor	54	45	40	28	130
Total CFU/mL	2700000	2300000	2000000	1500000	6500000
Inhibition (%)	58.46%	64.62%	69.23 %	76.92%	

[a] Control – the microorganism in DMSO only

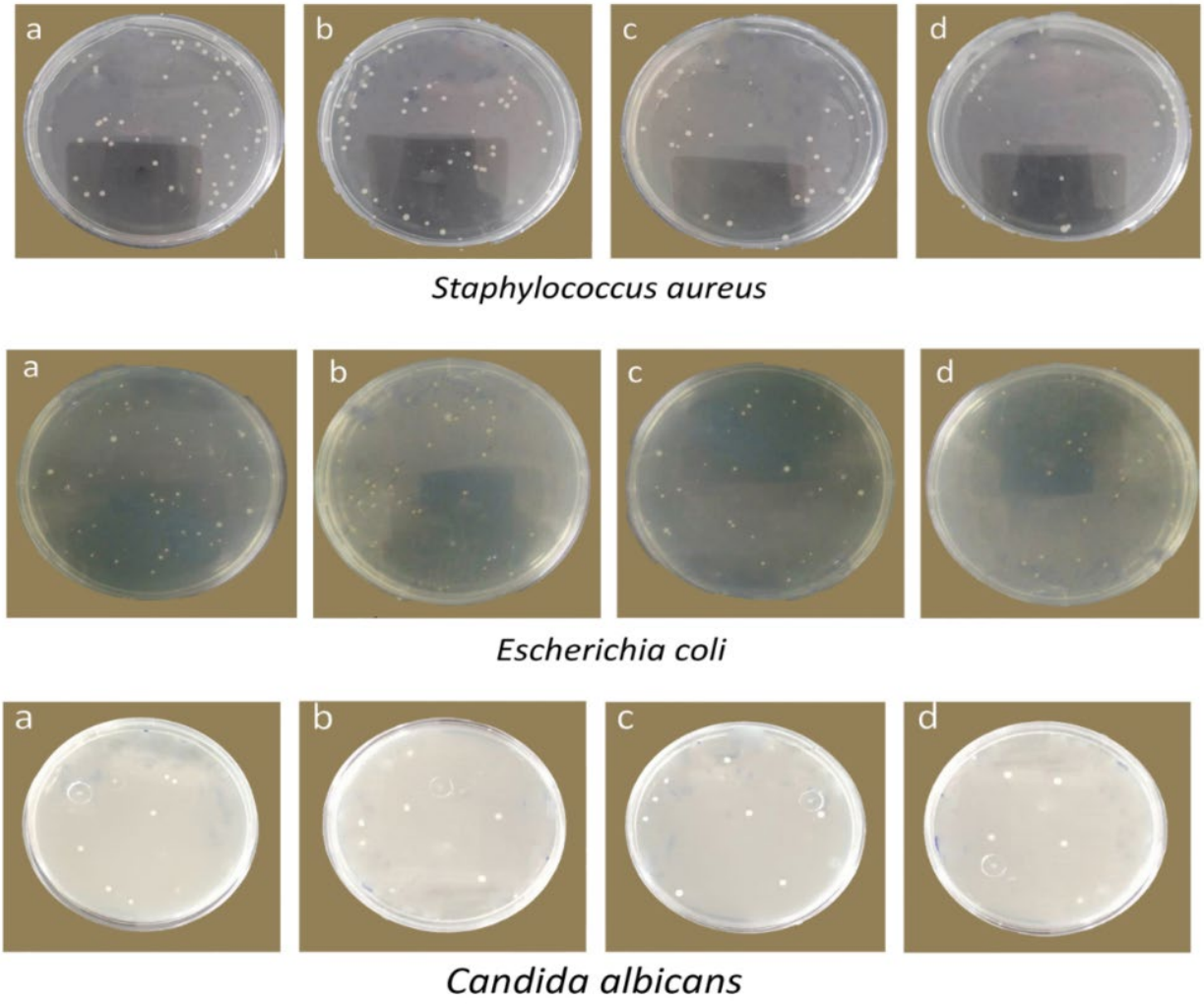

Figure 10: Photographs showing the antimicrobial activity of: (a) St-g-PMPA copolymer, (b) St-g-PMPA/PCL-3% hydrogel, (c) St-g-PMPA/PCL-3%/ZnONPs-1% composite and (d) St-g-PMPA/PCL-3%/ZnONPs-3% composite against proliferation of *S. aureus*, *E. coli* and *C. albicans*

Table 3
Antimicrobial activity of St-g-PMPA copolymer, St-g-PMPA/PCL-3% hydrogel and St-g-PMPA/PCL-3%/ZnONPs composites against *E. coli*

E. coli	St-g-PMPA	St-g-PMPA/PCL-3%	St-g-PMPA/PCL-3%/ZnONPs-1%	St-g-PMPA/PCL-3%/ZnONPs-3%	Control[a]
Dilution factor	10^{-4}	10^{-4}	10^{-4}	10^{-4}	10^{-4}
Volume of broth plated (µL)	20 µL	20 µL	20 µL	20 µL	20 µL
Colony forming unit (CFU) at the dilution factor	17	14	12	9	35
Total CFU/mL	850000	650000	600000	550000	1750000
Inhibition (%)	51.43%	62.86%	65.71%	68.57%	

[a] Control – the microorganism in DMSO only

Table 4
Antimicrobial activity of St-g-PMPA copolymer, St-g-PMPA/PCL-3% hydrogel and St-g-PMPA/PCL-3%/ZnONPs composites against *C. albicans*

C. albicans	St-g-PMPA	St-g-PMPA/PCL-3%	St-g-PMPA/PCL-3%/ZnONPs-1%	St-g-PMPA/PCL-3%/ZnONPs-3%	Control[a]
Dilution factor	10^{-3}	10^{-3}	10^{-3}	10^{-3}	10^{-3}
Volume of broth plated (µL)	20 µL	20 µL	20 µL	20 µL	20 µL
Colony forming unit (CFU) at the dilution factor	5	4	3	3	8
Total CFU/mL	126500	124500	111000	104500	300000
Inhibition (%)	57.83%	58.50%	63.00%	65.17%	

[a] Control – the microorganism in DMSO only

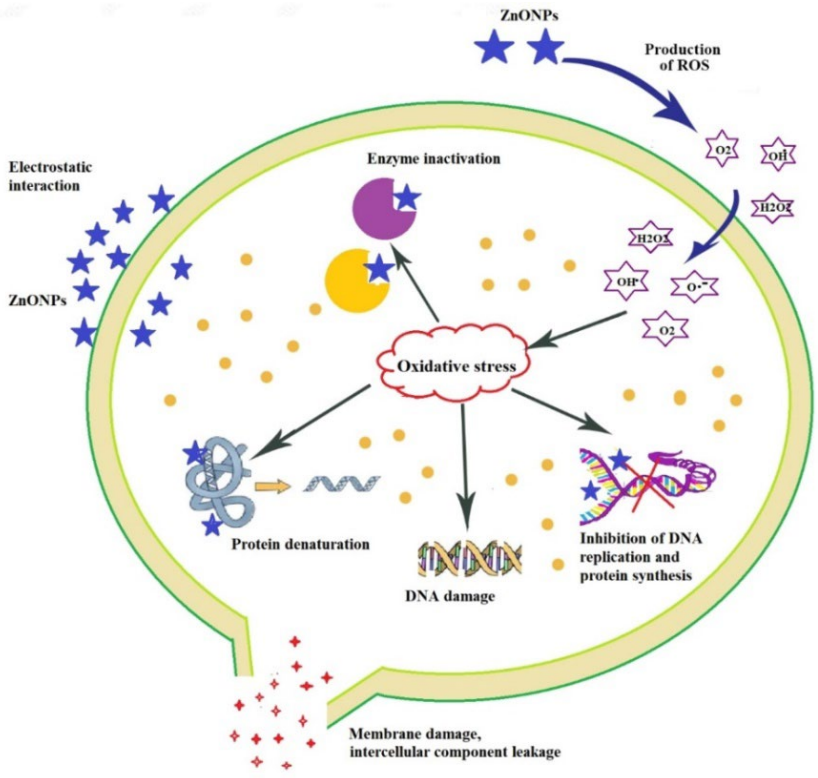

Figure 11: A schematic representation for the interaction between the ZnONPs and the microbial cell membrane

Preservation of green bell peppers

Green bell peppers have many benefits for humans, including antioxidants that protect the body from free radicals and oxidative stress. A single green bell pepper contains nearly 100% of the daily recommended amount of vitamin C, which supports a healthy immune system, promotes collagen production, maintains skin elasticity, and reduces signs of aging. The presence of vitamins A and E in green bell peppers helps to maintain eye health. Green bell peppers contain potassium, which can help regulating blood pressure and cholesterol levels. Their high fiber content promotes a healthy digestive system. Green bell peppers may help reduce inflammation in the body due to their antioxidants and vitamin C content.[44] Their preservation time varies depending on the storage method. The most common cause of pepper damage is improper handling and storage; biological, chemical, and physical factors all have an impact on their quality during these processes.

Green peppers that have been coated with an antimicrobial substance are protected from environmental damage and have a longer shelf life. Temperature, humidity, chilling, and microbiological contamination can significantly impact the quality and shelf life of fresh fruits after harvest. Edible coatings can prevent fruit from drying, reduce microbial contamination, and preserve its quality for longer periods of time. Polysaccharide-based coatings are effective gas obstructions due to their hydrophilic properties.[45]

St is the most frequently used polysaccharide in edible films and coatings due to its ability to form colorless, tasteless, and transparent layers with properties similar to synthetic polymers, including humidity, heat, and elasticity. These properties make starch-based edible films and coatings ideal for foodstuff packaging and preservation. It is safe and commonly used to preserve food.[6,46]

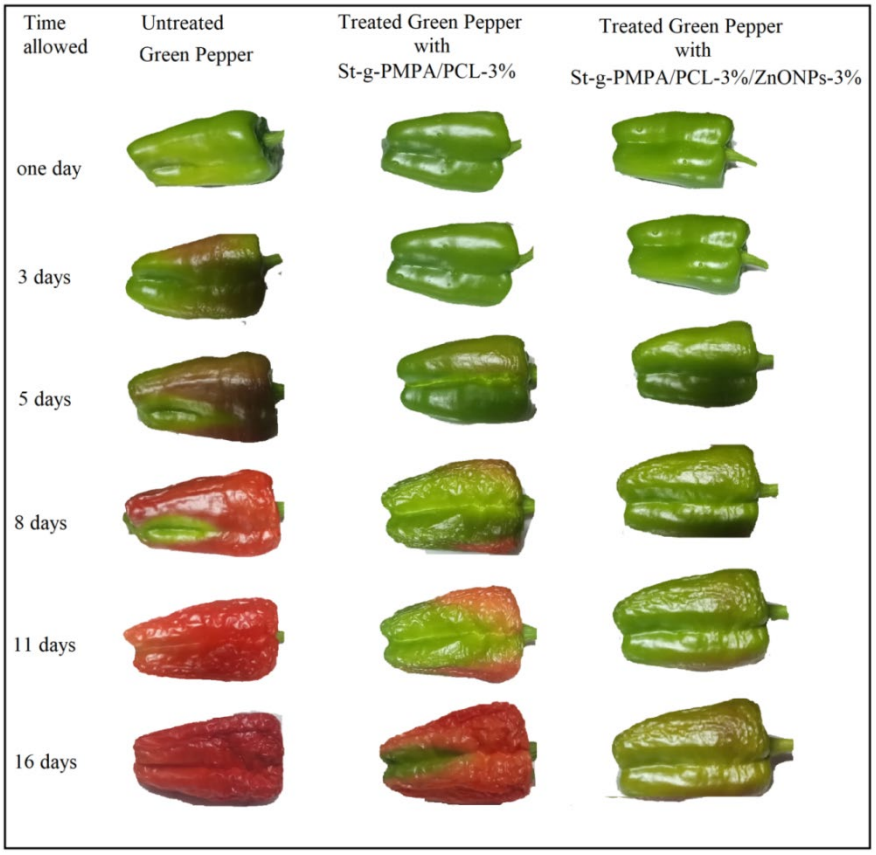

Figure 12: Photographs showing the preserving effect of the St-g-PMPA/PCL-3% hydrogel and St-g-PMPA/PCL-3%/ZnONPs-3% composite on green bell peppers

As shown in Figure 12, the St-g-PMPA/PCL-3% hydrogel and St-g-PMPA/PCL-3%/ZnONPs-3% composite (as an example of the prepared composites) were tested for the maintenance of green bell peppers under prevailing environmental conditions (open air at 30 °C). Fresh green bell peppers were coated with a suspended solution of modified St samples (62.5 μg mL^{-1}) using a spreading technique. To compare, uncoated green bell peppers were used under identical conditions. A digital camera was used to record the changes in shape and freshness of peppers over a period of 1-16 days.

We noticed that uncoated green bell peppers shrank in shape and lost weight, freshness, and green color faster than the coated ones. This could be due to the release of internal water and oxygen from peppers into the environment. In contrast, the coated ones retained their freshness, green color, and weight for an extended period of time. After 6 days of treatment, the pepper coated with the St-g-PMPA/PCL-3% hydrogel showed some changes in shape and freshness, whereas the pepper coated with the St-g-PMPA/PCL-3%/ZnONPs-3% composite showed an observable difference after 11 days. It appeared that the modified St had barrier properties that could protect the peppers from the harmful effects of elevated environmental temperature and humidity, thereby delaying the evaporation of water and gaseous components.

Thus, St-g-PMPA/PCL-3%/ZnONPs-3% was more potent in the preservation of the green bell peppers than the St-g-PMPA/PCL-3% hydrogel. This is due to the higher barrier effect of the ZnONPs, which can retard ripening and respiration during transit and storage. In addition, the antimicrobial activity of ZnONPs protects the peppers from microbial attack.[14,47]

Evaluation of cytotoxicity of St-g-PMPA/PCL-3%/ZnONPs-3% composite

The cytotoxicity of St-g-PMPA/PCL-3%/ZnONPs-3% composite (a representative example) was tested on normal human lung fibroblast cells (WI-38 cells line) at concentrations ranging from 0 to 500 μg/mL. The composite had no negative impact on cell viability at concentrations up to 15.6 μg/mL, but showed a slight inhibition effect of 1.93% at 31.25 μg/mL (Fig. 13).

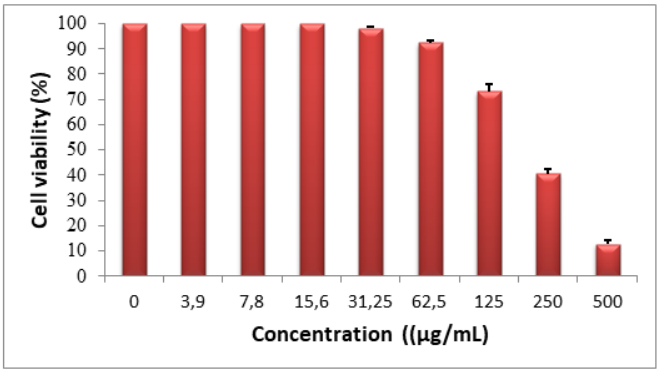

Figure 13: Cytotoxicity effect of St-g-PMPA/PCL-3%/ZnONPs-3% composite on WI-38 cell line

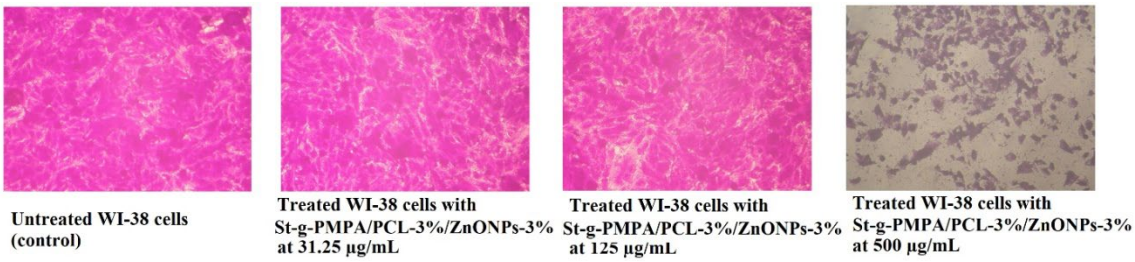

Figure 14: Microscopic analysis of WI-38 cell line after incubation for 24 h with St-g-PMPA/PCL-3%/ZnONPs-3% composite at concentrations of 31.25, 125 and 500 μg/mL, compared to the untreated cells (control cells)

At a concentration of 62.5 μg/mL, the cell viability was 92.56%, while at 500 μg/mL, it decreased to 12.69%. The cytotoxic concentration (CC_{50}), which affected 50% of intact cells,[48] was 213.84 ± 9.43 μg/mL. Thus, St-g-PMPA/PCL-3%/ZnONPs-3% composite could be an effective

antimicrobial agent for food and biomedical applications without destroying normal human cells at concentrations below 62.5 µg/mL. Figure 14 shows a microscopic exploration of WI-38 cell line that were incubated with St-g-PMPA/PCL-3%/ZnONPs-3% composite for 24 h at 31.25, 125, and 500 µg/mL concentrations, in comparison with the untreated normal cells.

CONCLUSION

St was chemically modified through the grafting/crosslinking process using MPA and different concentrations of CL crosslinker (3, 5, and 10% based on St weight) to yield three new St-g-PMPA/PCL-3%, St-g-PMPA/PCL-5%, and St-g-PMPA/PCL-10% hydrogels. Further, St-g-PMPA/PCL-3%/ZnONPs-1% and St-g-PMPA/PCL-3%/ZnONPs-3% composites were obtained by impregnating 1 and 3 wt% ratios of ZnONPs into the St-g-PMPA/PCL-3% hydrogel, respectively. Their surface topography, inner and chemical structure were investigated utilizing the proper analytical methods. As illustrated by the XRD and SEM investigation, the increase in the amount of the cross-linker (CL) from 3 to 5% and ZnONPs from 1 to 3% resulted in an increase in the amorphous parts and porosity in both of the resulting hydrogels and composites, due to the extensive breakage of greater amounts of the internal hydrogen bonds. The swellability of the St-g-PMPA/PCL hydrogels, at various pH (4, 7, and 9) over various time intervals at 25 °C, improved with increasing the amount of the incorporated cross-linker (CL) from 3 to 10%. Although the virgin St did not show any activity against the inspected microbes, the modification process significantly improved its antimicrobial behavior. It was found that St-g-PMPA/PCL-3%/ZnONPs composites possess greater antimicrobial activity, against all the tested microbes, compared to their parent St-g-PMPA/PCL-3% hydrogel, which, in its turn, showed better activity than its parent St-g-PMPA copolymer. Microbial inhibition increased with increasing the ZnONPs content from 1 to 3 wt%. Their order of antimicrobial activity was the following: St-g-PMPA/PCL-3%/ZnONPs-3% > St-g-PMPA/PCL-3%/ZnONPs-1% > St-g-PMPA/PCL-3% > St-g-PMPA. Further, their antimicrobial performance against Gram-positive bacteria was better than that against Gram-negative bacteria and fungi. Coating the green bell peppers with a thin layer of St-g-PMPA/PCL-3%/ZnONPs-3% composite led to spoilage retardation for a time period up to16 days. The St-g-PMPA/PCL-3%/ZnONPs-3% had no harming impact on the viability of normal human lung fibroblast cells (WI-38 cell line) at concentrations up to 15.6 µg/mL. Thus, an appreciable enhancement in the antimicrobial activity of St was achieved when MPA, CL, and ZnONPs were amalgamated into its matrix. This is a favorable enough strategy to provide some systems to serve as good alternatives for traditional antimicrobial agents in the biomedical and food preservation domains.

REFERENCES

[1] R. T. Alfuraydi, N. F. Al-Harby, F. M. Alminderej, N. Y. Elmehbad and N. A. Mohamed, *Gels*, **9**, 882 (2023), https://doi.org/10.3390/gels9110882

[2] R. T. Alfuraydi, F. M. Alminderej and N. A. Mohamed, *Polymers*, **14**, 1619 (2022), https://doi.org/10.3390/polym14081619

[3] N. H. Thang, T. B. Chien and D. X. Cuong, *Gels*, **9**, 523 (2023), https://doi.org/10.3390/gels9070523

[4] H. Choi, W.-S. Choi and J.-O. Jeong, *Gels*, **10**, 693 (2024), https://doi.org/10.3390/gels10110693

[5] N. A. Mohamed, N. F. Al-Harby and M. S. Almarshed, *Polym. Bull.*, **77**, 6135 (2020), https://doi.org/10.1007/s00289-019-03058-6

[6] N. Y. Elmehbad, N. A. Mohamed and N. A. Abd El-Ghany, *Starch-Stärke*, **76**, 2300258 (2024), https://doi.org/10.1002/star.202300258

[7] N. Y. Elmehbad, N. A. Mohamed, N. A. Abd EL-Ghany and M. M. Abd EL-Aziz, *Cellulose Chem. Technol.*, **56**, 983 (2022), https://doi.org/10.35812/CelluloseChemTechnol.2022.56.88

[8] M. H. Abu Elella, H. M. Abdallah, E. A. Ali, E. Makhado and N. A. Abd El-Ghany, *Int. J. Biol. Macromol.*, **304**, 140915 (2025), https://doi.org/10.1016/j.ijbiomac.2025.140915

[9] M. Salehi and A. Rashidinejad, *Int. J. Biol. Macromol.*, **290**, 138855 (2025), https://doi.org/10.1016/j.ijbiomac.2024.138855

[10] E. J. Murphy, G. W. Fehrenbach, I. Z. Abidin, C. Buckley, T. Montgomery *et al.*, *Polymers*, **15**, 2373 (2023), https://doi.org/10.3390/polym15102373

[11] Md. Qamruzzaman, F. Ahmed and Md. I. H. Mondal, *J. Polym. Environ.*, **30**, 19 (2022), https://doi.org/10.1007/s10924-021-02180-9

[12] X. Hou, H. Wang, Y. Shi and Z. Yue, *Carbohyd. Polym.*, **302**, 120392 (2023), https://doi.org/10.1016/j.carbpol.2022.120392

[13] J. Leong, C. Yang, J. Tan, B. Q. Tan, S. Hor *et al.*, *Biomater. Sci.*, **8**, 6920 (2020), https://doi.org/10.1039/D0BM00752H

[14] R. Rohani, N. S. F. Dzulkharnien, N. H. Harun and I. A. Ilias, *Bioinorg. Chem. Appl.*, **4**, 3077747 (2022), https://doi.org/10.1155/2022/3077747

[15] R. A. Alharbi, F. M. Alminderej, N. F. Al-Harby, N. Y. Elmehbad and N. A. Mohamed, *Polymers*, **15**, 980 (2023), https://doi.org/10.3390/polym15040980
[16] T. Majeed, A. H. Dar, V. K. Pandey, K. K. Dash, S. Srivastava *et al*., *Prog. Org. Coat*., **181**, 107597 (2023), https://doi.org/10.1016/j.porgcoat.2023.107597
[17] D. J. García-García, G. F. Pérez-Sánchez, H. Hernández-Cocoletzi, M. G. Sánchez-Arzubide, M. L. Luna-Guevara *et al*., *Polymers*, **15**, 3772 (2023), https://doi.org/10.3390/polym15183772
[18] H. Sharifan, A. Noori, M. Bagheri and J. M. Moore, *Crop Past. Sci*., **73**, 22 (2021), https://doi.org/10.1071/CP21191
[19] B. J. Arroyo, A. C. Bezerra, L. L. Oliveira, S. J. Arroyo, E. A. Melo *et al*., *Food Chem*., **309**, 125566 (2020), https://doi.org/10.1016/j.foodchem.2019.125566
[20] P. Purohit, A. Bhatt, R. K. Mittal, M. H. Abdellattif and T. A. Farghaly, *Front. Bioeng. Biotechnol*., **10**, 1044927 (2023), https://doi.org/10.3389/fbioe.2022.1044927
[21] N. A. Abd El-Ghany, M. S. Abdel-Aziz, M. M. Abdel Aziz and Z. M. Mahmoud, *Cellulose Chem. Technol*., **57**, 803 (2023), https://doi.org/10.35812/CelluloseChemTechnol.2023.57.71
[22] Y. Chen, G. Tian, B. Zhai, H. Zhang, Y. Liang *et al*., *Compos. B Eng*., **177**, 107416 (2019), https://doi.org/10.1016/j.compositesb.2019.107416
[23] N. A. Abd El-Ghany and Z. M. Mahmoud, *Polym. Bull*., **78**, 6161 (2021), https://doi.org/10.1007/s00289-020-03417-8
[24] B. Wu and D. J. Mcclements, *Food Hydrocoll*., **47**, 87 (2015), https://doi.org/10.1016/j.foodhyd.2015.01.021
[25] M. Bekhit, E. Arab-Tehrany, C. J. F Kahn, F. Cleymand, S. Fleutot *et al*., *Int. J. Mol. Sci*., **19**, 574 (2018), https://doi.org/10.3390/ijms19020574
[26] M. Shahbazi, M. Majzoobi and A. Farahnaky, *J. Food Eng*., **223**, 10 (2018), https://doi.org/10.1016/j.jfoodeng.2017.11.033
[27] E. Sharmin, M. T. Kafyah, A. A. Alzaydi, A. A. Fatani, F. A. Hazazzi *et al*., *Int. J. Biol. Macromol*., **163**, 2236 (2020), https://doi.org/10.1016/j.ijbiomac.2020.09.044
[28] A. V. Torres-Figueroa, C. J. Pérez-Martínez, T. D. Castillo-Castro, E. Bolado-Martínez, M. A. G. Corella-Madueño *et al*., *J. Chem*., 5860487 (2020), https://doi.org/10.1155/2020/5860487
[29] H. J. Kadri, F. Ahmed, M. H. Rahman and M. I. H. Modal, *Polym. Bull*., **82**, 7917 (2025), https://doi.org/10.1007/s00289-025-05840-1
[30] I. Ifmalinda, S. A. Kurnia and D. Cherie, *J. Appl. Agric. Sci. Technol*., **7**, 272 (2023), https://www.jaast.org/index.php/jaast/article/view/87
[31] N. Y. Elmehbad and N. A. Mohamed, *Int. J. Polym. Mater. Polym. Biomater*., **71**, 969 (2022), https://doi.org/10.1080/00914037.2021.1933975
[32] N. A. Mohamed, *Int. J. Biol. Macromol*., **276**, 133810 (2024), https://doi.org/10.1016/j.ijbiomac.2024.133810
[33] N. A. Mohamed and N. A. Abd El-Ghany, *Cellulose Chem. Technol*., **58**, 481 (2024), https://doi.org/10.35812/CelluloseChemTechnol.2024.58.45
[34] N. Y. Elmehbad, N. A. Mohamed and N. A. Abd El-Ghany, *Int. J. Biol. Macromol*., **205**, 719 (2022), https://doi.org/10.1016/j.ijbiomac.2022.03.076
[35] T. Mosmann, *J. Immunol. Methods*, **65**, 55 (1983), https://doi.org/10.1016/0022-1759(83)90303-4
[36] R. A. Alharbi, F. M. Alminderej, N. F. Al-Harby, N. Y. Elmehbad and N. A. Mohamed, *Polymers*, **15**, 1529 (2023), https://doi.org/10.3390/polym15061529
[37] N. A. Abd El-Ghany, M. S. Abdel Aziz, M. M. Abdel-Aziz and Z. Mahmoud, *Int. J. Biol. Macromol*., **134**, 912 (2019), https://doi.org/10.1016/j.ijbiomac.2019.05.078
[38] S. Faisal, H. Jan, S. A. Shah, S. Shah, A. Khan *et al*., *ACS Omega*, **6**, 9709 (2021), https://doi.org/10.1021/acsomega.1c00310
[39] J. C. Quintanilla de Stéfano, V. Abundis-Correa, S. D. Herrera-Flores and A. J. Alvarez, *Polymers*, **12**, 1974 (2020), https://doi.org/10.3390/polym12091974
[40] C. S. Lee and H. S. Hwang, *Gels*, **9**, 951 (2023), https://doi.org/10.3390/gels9120951
[41] Y. Xiang, X. Liu, C. Mao, X. Liu, Z. Cui *et al*., *Mater. Sci. Eng. C Mater. Biol. Appl*., **85**, 214 (2018), https://doi.org/10.1016/j.msec.2017.12.034
[42] M. R. Amiri, M. Alavi, M. Taran and D. Kahrizi, *J. Public Health Res*., **11**, 22799036221104151 (2022), https://doi.org/10.1177/22799036221104151
[43] N. A. Abd El-Ghany, M. H. Abu Elella, H. M. Abdallah, M. S. Mostafa and M. Samy, *J. Polym. Environ*., **31**, 2792 (2023), https://doi.org/10.1007/s10924-023-02798-x
[44] C. Chávez-Mendoza, E. Sanchez, E. Muñoz-Marquez, J. P. Sida-Arreola and M. A. Flores-Cordova, *Antioxidants* (*Basel*), **23**, 427 (2015), https://doi.org/10.3390/antiox4020427
[45] N. Y. Elmehbad and N. A. Mohamed, *Int. J. Polym. Mater. Polym. Biomater*., **71**, 1369 (2022), https://doi.org/10.1080/00914037.2021.1963724
[46] H. D. Almutairi, M. Abdel-Motaal, M. Sharaky and N. A. Mohamed, *Polymers*, **17**, 1061 (2025), https://doi.org/10.3390/ polym17081061
[47] N. Y. Elmehbad, N. A. Mohamed, N. A. Abd El-Ghany and M. M. Abdel-Aziz, *Int. J. Biol. Macromol*., **246**, 125582 (2023), https://doi.org/10.1016/j.ijbiomac.2023.125582
[48] M. Abdel-Motaal, D. A. Aldakhili, A. A. Elmaaty, M. Sharaky, M. A. E. Mourad *et al*., *Drug Dev. Res*., **85**, e22197 (2024), https://doi.org/10.1002/ddr.22197